



The influence of co-formers on the dissolution rates of co-amorphous sulfamerazine/excipient systems

Title	The influence of co-formers on the dissolution rates of co-amorphous sulfamerazine/excipient systems
Author(s)	Gniado, Katarzyna;Löbmann, Korbinian;Rades, Thomas;Erxleben, Andrea
Publication Date	2016-03-16
Publisher	Elsevier

The influence of co-formers on the dissolution rates of co-amorphous sulfamerazine/excipient systems

Katarzyna Gniado^a, Korbinian Löbmann^b, Thomas Rades^b, Andrea Erxleben^{a,*}

^a School of Chemistry, National University of Ireland, Galway, Ireland

^b Department of Pharmacy, University of Copenhagen, Copenhagen 2100, Denmark

ABSTRACT

A comprehensive study on the dissolution properties of three co-amorphous sulfamerazine/excipient systems, namely sulfamerazine/deoxycholic acid, sulfamerazine/citric acid and sulfamerazine/sodium taurocholate (SMZ/DA, SMZ/CA and SMZ/NaTC; 1:1 molar ratio), is reported. While all three co-formers stabilize the amorphous state during storage, only co-amorphization with NaTC provides a dissolution advantage over crystalline SMZ and the reasons for this were analyzed. In the case of SMZ/DA extensive gelation of DA protects the amorphous phase from crystallization upon contact with buffer, but at the same time prevents the release of SMZ into solution. Disk dissolution studies showed an improved dissolution behavior of SMZ/CA compared to crystalline SMZ. However, enhanced dissolution properties were not seen in powder dissolution testing due to poor dispersibility. Co-amorphization of SMZ and NaTC resulted in a significant increase in dissolution rate, both in powder and disk dissolution studies.

Keywords: co-amorphization, dissolution studies, dispersibility, sulfamerazine

* Corresponding author. Tel.: +353 91 492487. Fax: +353 91 495576.

School of Chemistry, NUI Galway, University Road, Galway Ireland

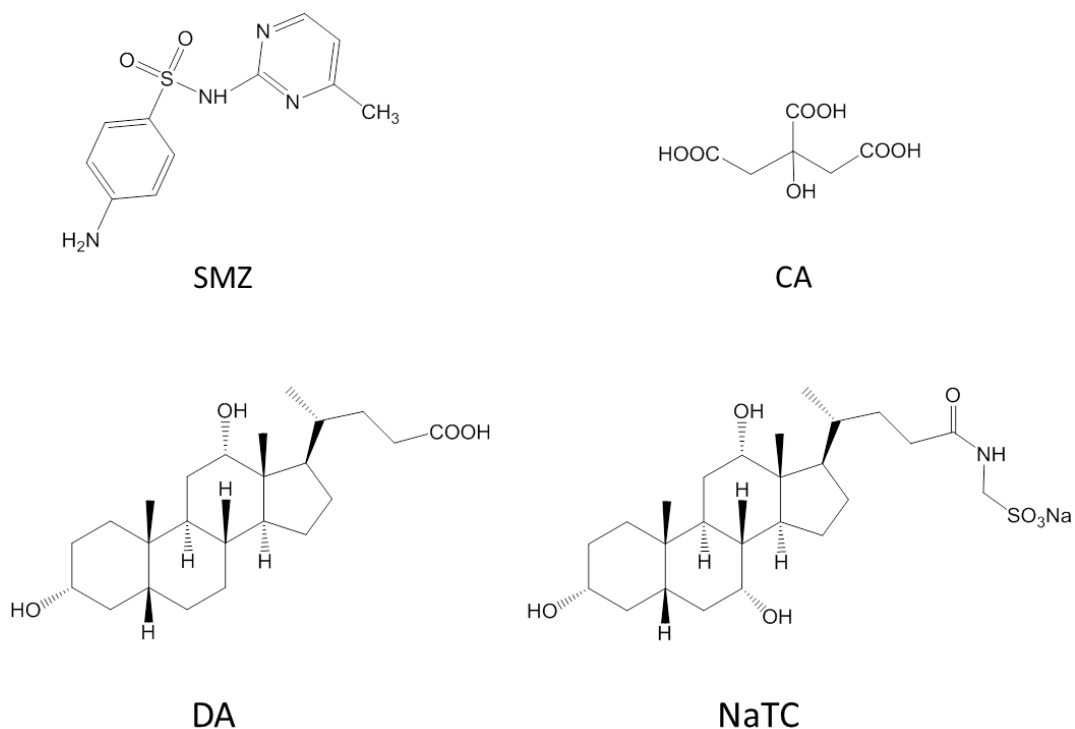
E-mail address: andrea.erxleben@nuigalway.ie (A. Erxleben).

1. Introduction

Low aqueous solubility leading to poor bioavailability is one of the major hurdles in drug development to date. It has been estimated that up to 75 % of the drugs in the development pipeline are classified as BCS class II drugs, i.e. poorly soluble (Williams, 2013). An attractive, yet challenging approach to overcome poor water solubility is to convert a crystalline active pharmaceutical ingredient (API) into its amorphous form that possesses a higher apparent solubility and dissolution rate than the crystalline form. However, the amorphous form represents a high energy form with inherently low physical stability. As a consequence, recrystallization during manufacturing, storage, or dissolution restricts the use of amorphous drug compounds.

Recently, the formation of co-amorphous stoichiometric mixtures, consisting of either an API and a low molecular weight excipient or two active drug substances, have been shown to be a promising strategy to stabilize the amorphous form of a drug and to date a number of co-amorphous systems with enhanced physicochemical properties have been prepared by co-milling or quench-cooling (Chieng et al., 2009; Allesø et al., 2009; Löbmann et al., 2011; Löbmann et al., 2012; Lu et al., 1998; Masuda et al., 2012; Hoppu et al., 2007; Hoppu et al., 2009). The increased stability is generally attributed to intermolecular interactions such as hydrogen bonding between the API and the co-former or between the two APIs.

We have recently studied the milling-induced amorphization of the model API sulfamerazine (SMZ) and demonstrated that co-milling with multifunctional carboxylic acids such as citric acid (CA) can increase the stability of the amorphous phase under ambient conditions from a few hours for the drug alone to several weeks (MacFhionnghaile et al., 2014). In continuation of this work we now report a detailed study of the dissolution behavior of three selected co-amorphous SMZ/carboxylic acid co-former systems, namely SMZ/DA, SMZ/CA and SMZ/NaTC (DA = deoxycholic acid, NaTC = sodium taurocholate, Scheme 1). DA and NaTC were chosen as examples for bile acids and bile acid salts. Bile acids are synthesized in the liver and their salts have been studied as solubilizers and nucleation inhibitors due to their micelle-forming properties (Chen, Mosquera-Giraldo et al., 2015; Chen, Ormes et al., 2015). While SMZ and DA have comparable aqueous solubility, CA and NaTC represent co-formers that are readily soluble in water. It was hoped to reveal whether a rapidly dissolving co-former will help the dissolution of SMZ or actually hinder it, as SMZ is “left behind”, while a less soluble and more slowly dissolving co-former enables a more controlled concurrent dissolution by “taking the API along”.



Scheme 1. Chemical structures of sulfamerazine (SMZ), citric acid (CA), deoxycholic acid (DA) and sodium taurocholate (NaTC).

2. Materials and methods

2.1. Materials

SMZ (form I, purity $\geq 99.0\%$), DA (purity $\geq 99.0\%$), CA (purity $\geq 99.0\%$) and amorphous NaTC (purity $\geq 98.0\%$) were purchased from Sigma Aldrich (St. Louis, Missouri) and were used as received. The polymorphic form I of the commercial sample of SMZ and the amorphous form of commercial sodium taurocholate were confirmed by X-ray powder diffraction (XRPD).

2.2. Methods

2.2.1. Preparation of amorphous DA and SMZ

DA (1 g) was milled for 60 min at 25 Hz in a 25-mL stainless steel jar containing one 15-mm stainless steel ball using an oscillatory ball mill (Mixer Mill MM400; Retsch GmbH, Haan, Germany). To avoid overheating of the sample a break of 15 min was taken after 30 min of milling. For the preparation of amorphous SMZ, the milling jars containing 1 g of SMZ form I were sealed and immersed in liquid nitrogen for 3 min before milling for 60 min. Every 7.5 min, the milling jars were re-cooled with

liquid nitrogen for 2 min. The average sample temperature measured at 7.5 min intervals was $-10 \pm 2^\circ\text{C}$. The formation of amorphous SMZ and DA was confirmed by XRPD.

2.2.2. Preparation of co-amorphous SMZ/DA, SMZ/CA and SMZ/NaTC

Co-amorphous SMZ/DA, SMZ/CA and SMZ/NaTC were prepared by cryomilling equimolar mixtures of SMZ with DA, CA or NaTC (1 g total) for 120 min using the method outlined above for the preparation of amorphous SMZ. The conversion to the amorphous form was confirmed by XRPD.

2.2.3. X-ray powder diffraction

X-ray powder patterns were recorded on an Inel Equinox 3000 powder diffractometer (Artenay, France) between 5 and 90° (2θ) using $\text{Cu K}\alpha$ radiation ($\lambda = 1.54178 \text{ \AA}$, 35 kV, 25 mA).

2.2.4. Attenuated total reflectance infrared spectroscopy

Attenuated total reflectance infrared (ATR-IR) spectra were recorded from 4000 to 650 cm^{-1} using a PerkinElmer Spectrum 400 (FT-IR/FT-NIR spectrometer, Waltham, Massachusetts) with 32 accumulations at a resolution of 4 cm^{-1} . This instrument was equipped with a DATR 1 bounce Diamond/ZnSe Universal ATR sampling accessory.

2.2.5. Near-infrared spectroscopy

Near-infrared (NIR) spectra were collected in glass vials ($15 \times 45 \text{ mm}^2$) on a PerkinElmer Spectrum One (Waltham, Massachusetts) fitted with an NIR reflectance attachment. Spectra were collected with interleaved scans in the $10,000\text{--}4000 \text{ cm}^{-1}$ range with a resolution of 8 cm^{-1} using 32 co-added scans.

2.2.6. Dissolution studies

For the disc dissolution testing the powder samples were compressed into disks of 13 mm diameter using a hydraulic press (PerkinElmer, Model D7770, Ueberlingen, Germany). Crystalline or amorphous SMZ (100 mg), co-amorphous SMZ/DA (250 mg), co-amorphous SMZ/CA (170 mg) and co-amorphous SMZ/NaTC (300 mg) were compressed at a pressure of 7.5 MPa for 10 s, resulting in a compact disc with a flat circular surface. XRPD patterns were recorded to confirm that no crystallization had taken place during compression. The compact disc was placed in 250 mL 0.1 M phosphate buffer (pH 6.8, 37°C) and stirred using an 11-mm magnetic stirring bar at 300 rpm. Aliquots of 2.5 mL were withdrawn at predetermined time points (2, 4, 6, 10, 15, 20, 30, and 45 min) and immediately replaced with 2.5 mL of dissolution medium. The samples were diluted by addition of 4.75 mL dissolution medium and analyzed the same day using UV/Vis spectroscopy as described below. All dissolution experiments were conducted in triplicate.

For the powder dissolution studies powder samples of SMZ (100 mg, crystalline or amorphous), co-amorphous SMZ/DA (250 mg), co-amorphous SMZ/CA (170 mg) or co-amorphous SMZ/NaTC (300 mg) were weighed out, placed in 250 mL 0.1 M phosphate buffer (pH 6.8, 37°C) and stirred at 300 rpm using an 11-mm magnetic stirring bar. Aliquots of 2.5 mL were withdrawn at predetermined time points (2, 5, 10, 15, 25, 30, 45, 60, 90, 120, and 180 min) and immediately replaced with 2.5 mL of dissolution medium. The samples were diluted by addition of 4.75 mL dissolution medium and analyzed the same day using the UV/Vis method described below. All dissolution experiments were carried out in triplicate.

The amount of the dissolved SMZ was determined by UV/Vis spectroscopy using a Varian Cary 50 Scan Spectrophotometer (Santa Clara, CA, USA). Reference spectra were recorded for the buffer solution and the buffer solution containing either DA, CA or NaTC, in the range from 200 to 500 nm, in order to exclude any interference with the SMZ absorption in this range. The SMZ concentrations were measured at 258 nm. Standard solutions (50.95, 38.20, 25.48, 12.74, 5.95, 2.54, 1.27 and 0.51 µg/mL SMZ) were prepared in phosphate buffer (0.1 M, pH 6.8). The resulting calibration curve was linear in the relevant concentration range ($R^2 = 0.9984$).

To check for recrystallization of amorphous SMZ and SMZ/DA samples during dissolution testing, powder samples (approximately 0.2 g) were suspended in the solution medium (10 mL 0.1 M phosphate buffer, pH 6.8), stirred for different time intervals, filtered, air-dried and immediately analyzed by XRPD. Care was taken to filter and dry the samples as quickly as possible to avoid crystallization during drying. Similarly, compacted samples were placed in buffer. At different time intervals the disk was removed, dried with filter paper and placed on a sample holder for XRPD analysis.

3. Results and discussion

3.1. Preparation and characterization of the co-amorphous systems

Co-amorphous SMZ/CA was prepared by cryomilling an equimolar mixture of SMZ and CA and characterized by XRPD as previously described by us (MacFhionnghaile et al., 2014). Co-amorphous SMZ/DA and SMZ/NaTC were obtained in the same way in the present study. No crystalline peaks were observed in the XRPD patterns of SMZ/DA and SMZ/NaTC after storage at 4 °C in sealed vials for 4 months (Fig. 1). SMZ/CA remained X-ray amorphous for 7 d, but showed sharp diffraction peaks of SMZ form II after 14 d (MacFhionnghaile et al., 2014). No citric acid peaks were observed. By contrast, amorphous SMZ on its own crystallizes to form II within hours when kept at room temperature.

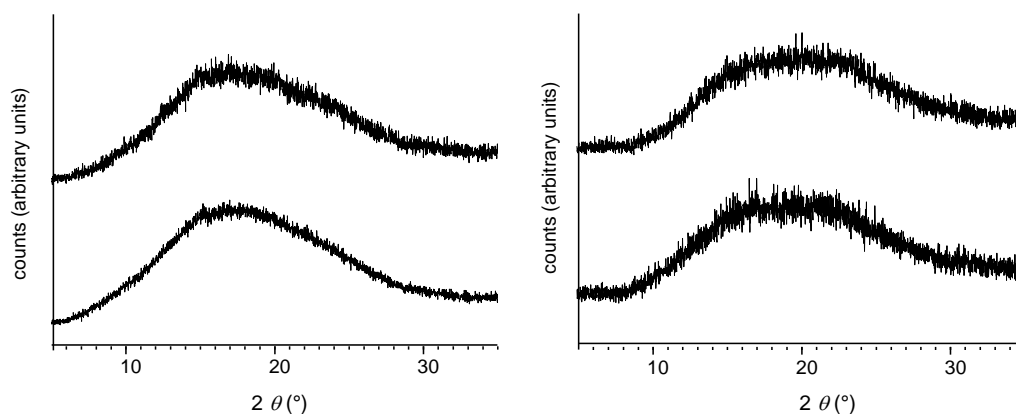


Fig. 1. XRPD patterns of (a) SMZ/DA and (b) SMZ/NaTC after cryomilling for 120 min (bottom) and after storage at 4 °C in a sealed vial for 4 months (top).

A comparison of the vibrational spectra of SMZ/DA, amorphous SMZ and amorphous DA showed slight band shifts of $\leq 3 \text{ cm}^{-1}$ in the IR region and more pronounced changes in the $5700 - 7000 \text{ cm}^{-1}$ and $4100 - 5200 \text{ cm}^{-1}$ ranges of the NIR region (Fig. S1a, Supporting Information). The $5700 - 7000 \text{ cm}^{-1}$ and $4100 - 5200 \text{ cm}^{-1}$ regions encompass the first overtones of the N-H stretching vibrations and the combination bands of N-H stretching and NH_2 bending vibrations, respectively, and are more sensitive to changes in H bonding interactions than bands in the IR region. The most prominent shifts are observed for the SMZ bands at 6580 and 5078 cm^{-1} and the DA band at 5814 cm^{-1} that move to 6586 , 5084 and 5806 cm^{-1} upon co-amorphization. It should be noted that these shifts are below the resolution limit of the NIR spectra. However, they occur repeatedly after multiple sampling which suggests that they are significant. In contrast to DA, NaTC has a sulfonate functional group that represents a strong H bond acceptor due to its negative charge resulting in more pronounced changes in the IR spectrum compared to SMZ/DA. The $\nu_{\text{as}}(\text{SO}_3^-)$ bands of NaTC appear at 1163 and 1039 cm^{-1} in the IR spectrum of the pure amorphous salt and at 1151 and 1042 cm^{-1} in that of SMZ/NaTC suggesting H bonding interactions with SMZ. The amide band of NaTC at 1637 cm^{-1} shifts to lower wavenumbers and is probably buried under the broad SMZ band at 1632 cm^{-1} . The NIR spectrum of SMZ/NaTC (Fig. S1b, Supporting Information) gives further evidence of strong intermolecular interactions between SMZ and NaTC. Co-amorphization leads to a shift of the SMZ bands at 5078 and 4539 cm^{-1} to 5085 and 4534 cm^{-1} . By contrast, no spectroscopic evidence for significant interactions between SMZ and CA could be obtained (MacFhionnghaile et al., 2014).

3.2. Dissolution studies of amorphous SMZ

Dissolution studies were carried out on disks of compacted powder and on powder samples under sink conditions. The disk dissolution profiles of amorphous and crystalline SMZ are shown in Fig. 2a.

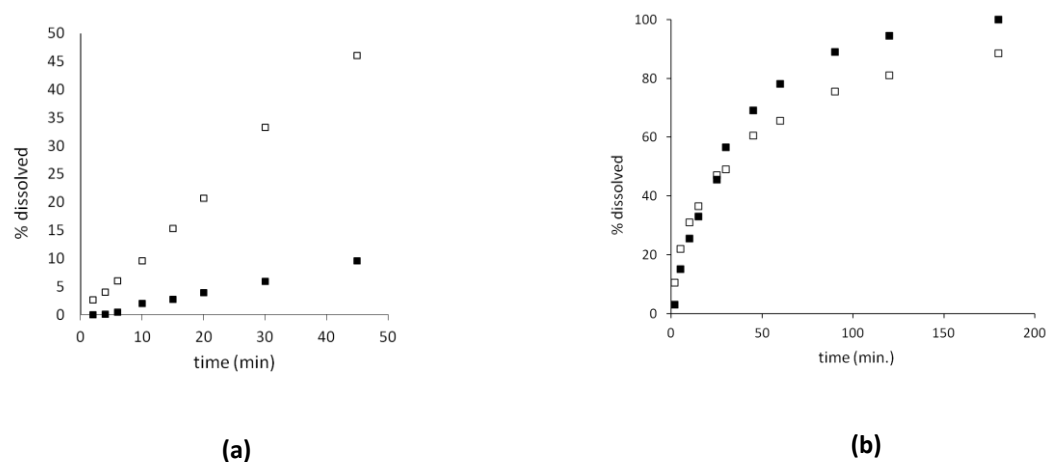


Fig. 2. Disk dissolution profile (a) and powder dissolution profile (b) of amorphous (□) and crystalline (■) SMZ. Phosphate buffer (pH 6.8), 37 °C.

The percentage of dissolved SMZ increases linearly with time and as expected, the dissolution rate of the amorphous phase is significantly higher than that of the crystalline phase. After 45 min, 46.1 % of the amorphous SMZ has dissolved compared to 9.6 % for crystalline SMZ. By contrast, the powder dissolution profile of amorphous SMZ over 3 h is very similar to that of the crystalline form (Fig. 2b). After 180 min. amorphous and crystalline SMZ are almost fully dissolved. To check for solvent-mediated recrystallization, a powder sample was suspended in buffer and after different time intervals samples were taken, filtered, dried and analyzed by XRPD (Fig. S2a, Supporting Information). Crystalline peaks of SMZ form II were observed after 2 min. indicating that crystallization to the most stable polymorph takes place in solution. Furthermore, during the powder dissolution testing significant clumping of the powder was observed. This severely reduces the accessible area for dissolution of the SMZ, and thus results in a reduced dissolution rate according to the Noyes-Whitney equation (Noyes and Whitney, 1897). When crystallization occurs on the surface of the clumps, the amorphous inner part is prevented from dissolution. Crystallization of form II also took place during the disk dissolution testing, albeit at a slower rate than in the case of the powder sample. While the powder had almost completely crystallized after 2 min., the diffractograms of the compacted sample showed a pronounced underlying amorphous halo for at least 10 min (Fig. S2b, Supporting Information).

3.3. Dissolution studies of co-amorphous SMZ/DA

The disk dissolution profile displayed in Fig. 3 shows that SMZ is released very slowly from co-amorphous SMZ/DA. After 45 min. 5.6 % of the SMZ has dissolved corresponding to a concentration that is almost eight times lower than in the case of amorphous SMZ in the absence of DA ($22.5 \mu\text{g mL}^{-1}$ vs. $184.4 \mu\text{g mL}^{-1}$). In fact, the dissolution advantage over crystalline SMZ is completely lost in the case of the co-amorphous system and the percentage dissolved after 45 min is even slightly lower than for crystalline SMZ (9.6 %). Likewise, the powder dissolution profile does not differ significantly from that of the crystalline API (Fig. S3, Supporting Information).

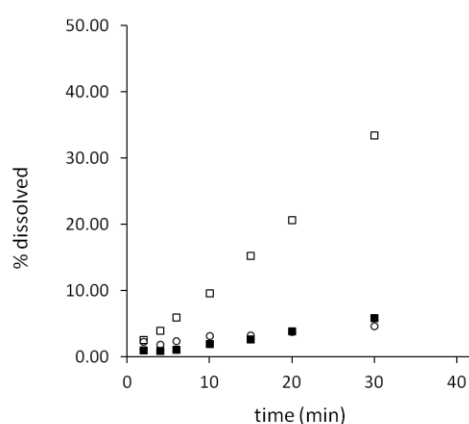


Fig. 3. Disk dissolution profiles of crystalline SMZ (■), amorphous SMZ (□) and amorphous SMZ in co-amorphous SMZ/DA (○) in phosphate buffer (pH 6.8, 37 °C).

In contrast to pure SMZ, the powder sample remained almost fully X-ray amorphous on contact with buffer for up to 60 min (Fig. 4). However, clumping of the powder was observed which offsets the dissolution enhancement of the amorphous form. Rationalizing the poor disk dissolution properties of SMZ/DA is less obvious. As described above, intermolecular interactions between the drug molecule and co-former are usually considered to be the reason for the higher stability of co-amorphous systems towards crystallization compared to the pure amorphous drug. To investigate whether intermolecular interactions between SMZ and DA affect the release of SMZ into solution, SMZ and DA were cryomilled separately and the dissolution behavior of a 1:1 physical mixture of the amorphous compounds was studied. The disk dissolution profile of the physical mixture is very similar to that of the co-amorphous system (Fig. S4, Supporting Information). From the percentage of dissolved SMZ reached over 45 min that is even slightly lower in the case of the physical mixture

(3.1 vs. 5.6 %) it is clear that SMZ-DA interactions are not the reason for the poor dissolution properties of co-amorphous SMZ/DA.

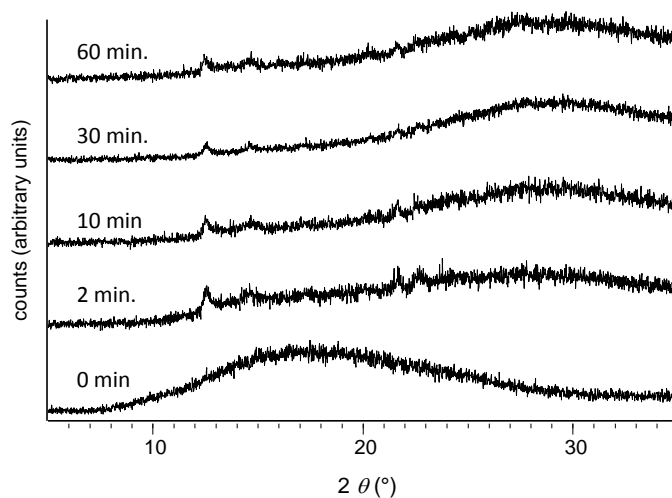


Fig 4. XRPD patterns of powder samples of co-amorphous SMZ/DA suspended in phosphate buffer (pH 6.8) for the times indicated.

After being subjected to the dissolution study the disk of co-amorphous SMZ/DA was covered with a gel. The same was observed for the physical mixture of separately cryomilled SMZ and DA. On drying in air, the gel-like surface converted to a solid that could be scraped off and be analyzed by XRPD. The XRPD pattern displayed the characteristic peaks of polymorph I of SMZ (Fig. 5). By contrast, the material inside the disk gave an amorphous halo indicating that the gel-like surface protects the amorphous phase from water and thus from crystallization, but at the same time prevents disintegration and hinders dissolution. The gel presents a diffusion layer through which SMZ needs to diffuse which can explain the similar dissolution rates of the co-amorphous system and the physical mixture.

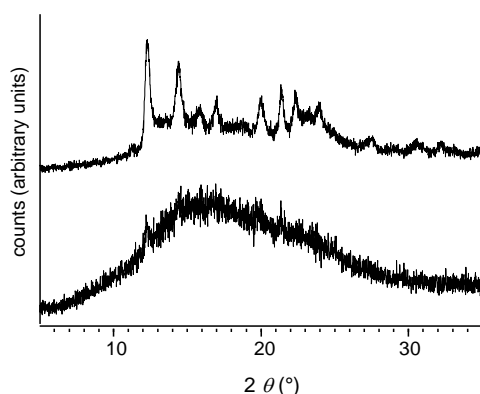


Fig. 5. XRPD patterns of the surface of the SMZ/DA disk used in the dissolution study after drying (top) and of the inner part of the disk (bottom).

Gel formation was also observed, when disks of pure cryomilled (amorphous) DA were exposed to buffer solution (Fig. 6). Noteworthy, this was not the case for crystalline DA. The tendency of certain bile acids to gelation and the dependence of the degree and rate of gelation on the pH value and the concentration have been described in the literature (Sobotka and Czczowiczka, 1958). Particle size reduction and amorphization during cryomilling enhances the reactivity and molecular mobility, and may thus accelerate the gelation, while in the case of crystalline DA, the gelation is slower and does not occur in the course of the study.

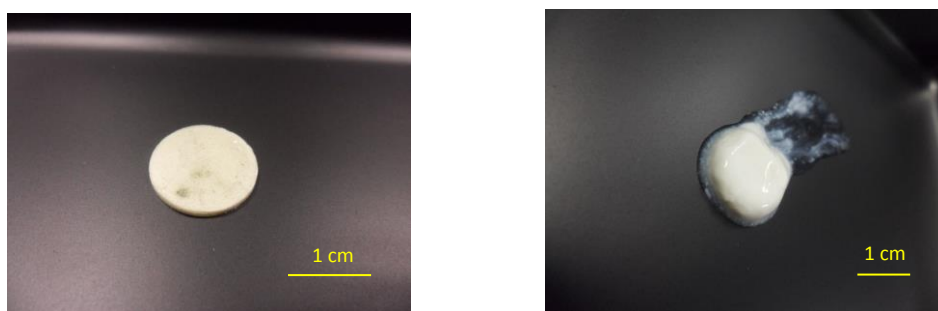


Fig. 6. Surface of a cryomilled DA disk before (left) and after 6 h in phosphate buffer (pH 6.8).

3.4. Dissolution studies of co-amorphous SMZ/CA

The disk dissolution profile of SMZ/CA (Fig. 7a) showed that co-amorphization of SMZ with CA leads to an improved dissolution behavior compared to crystalline SMZ. By contrast, no dissolution

advantage over the crystalline form is observed, when amorphous SMZ is physically mixed with cryomilled CA. In the case of the physical mixture 6.9 % of the SMZ had dissolved after 45 min compared to 29.3 % for the co-amorphous mixture. The dissolved percentage of the physical mixture is even slightly lower than that obtained for crystalline SMZ within the same time (9.6 %). The fact that amorphous SMZ physically mixed with CA does not exhibit the same disk dissolution behavior as pure amorphous SMZ (46.1 % dissolved after 45 min) is worthy of discussion. Citric acid on its own does not amorphize on cryomilling. Thus, crystalline CA particles in the physical mixture may act as crystallization promoters. However, CA is highly soluble and is expected to dissolve rapidly so that potential crystallization seeds may not be present for long enough. On the other hand, the surface area of the disk occupied by SMZ is lower for SMZ/CA disks than for pure SMZ disks which has to be taken into account as a factor contributing to the observed difference in dissolution rate.

In contrast to the disk dissolution study, enhanced dissolution properties of co-amorphous SMZ/CA were not seen in powder dissolution testing (Fig. 7b). As in the case of SMZ alone, this is due to a lack of dispersibility. The powder clumped on the surface of the solution and sank slowly to the bottom as a clump. However, despite the reduced accessible surface area, the powder still dissolves at a rate similar to that of crystalline SMZ in line with the higher intrinsic dissolution rate of SMZ/CA.

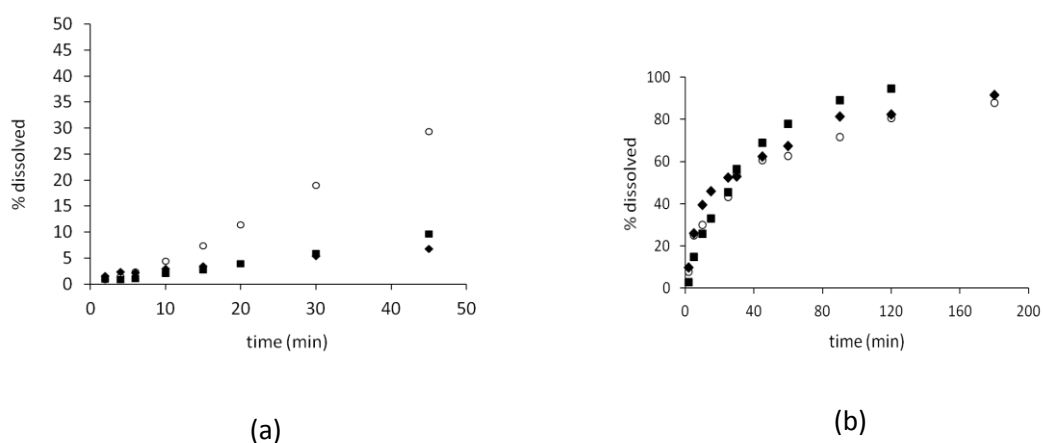


Fig. 7. Disk dissolution profiles (a) and powder dissolution profiles (b) of SMZ in co-amorphous SMZ/CA (O), of amorphous SMZ physically mixed with cryomilled CA (◆) and of crystalline SMZ (■). Phosphate buffer (pH 6.8), 37 °C.

3.5. Dissolution studies of co-amorphous SMZ/NaTC

As described above, co-amorphous SMZ/DA shows excellent stability towards recrystallization, both in the solid state and in solution, but has poor dissolution properties due to gel formation. Sobotka and Czczowicka have compared the propensity of different bile acids to gelation and associated the phenomenon with a specific molecular architecture (Sobotka and Czczowiczka, 1958). The “lower side” of DA presents a line of (unsubstituted) methylene groups allowing unhindered van der Waals attraction. By contrast, bile acids that have polar groups on both “sides” do not form gels. This led us to selecting NaTC (Scheme 1) as a bile acid co-former. In addition, due to the presence of the sulfonate group, NaTC is fully ionized at pH 6.8 (pK_a of TC = 1.9) and thus has a higher solubility compared to DA (pK_a = 6.5) at the pH of the dissolution studies. Rapid dissolution was observed in both the disk dissolution and the powder dissolution testing. The powder sample dispersed and dissolved almost instantaneously and powder and disk showed a clear dissolution advantage for co-amorphous SMZ/NaTC over crystalline SMZ (Fig. 8).

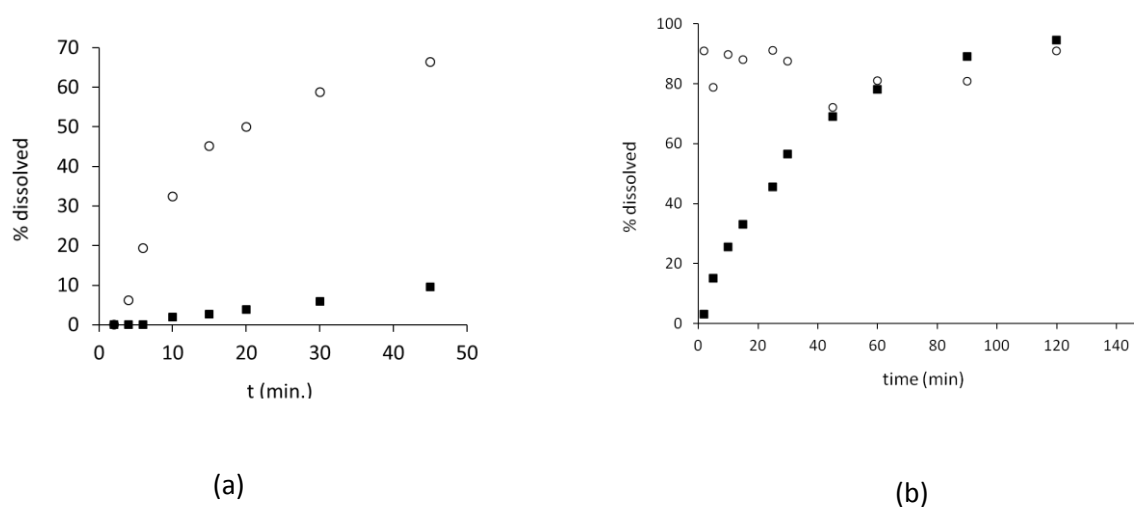


Fig. 8. Disk dissolution (a) and powder dissolution profiles (b) of SMZ in co-amorphous SMZ/NaT (○) and of crystalline SMZ (■). Phosphate buffer (pH 6.8), 37 °C.

4. Conclusions

Co-amorphisation of SMZ with CA and DA stabilizes the amorphous form in the solid state. However, powder dissolution studies indicated that neither of the two co-amorphous systems showed the expected dissolution advantage over crystalline SMZ. The slow dissolution kinetics of SMZ/CA are

due to a dispersion problem. Although SMZ/DA is highly stable towards recrystallization during storage, it is unsuitable as a formulation due to surface gelation that hinders drug release. By contrast, NaTC enhances the stability as well as the dissolution properties.

In conclusion the study shows that in the development of co-amorphous formulations, good dispersibility of the formulation is an important factor besides the prevention of crystallization.

Acknowledgement

This work was supported by Science Foundation Ireland under Grant No. [07/SRC/B1158] as part of the Synthesis and Solid State Pharmaceutical Centre (SSPC).

References

Allesø, M., Chieng, N., Rehder, S., Rantanen, J., Rades, T., Aaltonen, J., 2009. Enhanced dissolution rate and synchronized release of drugs in binary systems through formulation: amorphous naproxen-cimetidine mixtures prepared by mechanical activation. *J. Control. Release* 136, 45–53.

Chen, J., Mosquera-Giraldo, L.I., Ormes, J.D., Higgins, J.D., Taylor, L.S., 2015. Bile salts as crystallization inhibitors of supersaturated solutions of poorly water-soluble compounds. *Cryst. Growth Des.* 15, 2593–2597.

Chen, J., Ormes, J.D., Higgins, J.D., Taylor, L.S., 2015. Impact of surfactants on the crystallization of aqueous suspensions of celecoxib amorphous solid dispersion spray dried particles. *Mol. Pharmaceutics* 12, 533–541.

Chieng, N., Aaltonen, J., Saville, D., Rades, T., 2009. Physical characterization and stability of amorphous indomethacin and ranitidine hydrochloride binary systems prepared by mechanical activation. *Eur. J. Pharm. Biopharm.* 71, 47–54.

Hoppu, P., Jouppila, K., Rantanen, J., Schantz, S., Juppo, A.M., 2007. Characterisation of blends of paracetamol and citric acid. *J. Pharm. Pharmacol.* 59, 373–381.

Hoppu, P., Hietala, S., Schantz, S., Juppo, A.M., 2009. Rheology and molecular mobility of amorphous blends of citric acid and paracetamol. *Eur. J. Pharm. Biopharm.* 71, 55–63.

Löbmann, K., Laitinen, R., Grohganz, H., Gordon, K.C., Strachan, C., Rades, T., 2011. Coamorphous drug systems: enhanced physical stability and dissolution rate of indomethacin and naproxen. *Mol. Pharmaceutics*. 8, 1919–1928.

Löbmann, K., Strachan, C., Grohganz, H., Rades, T., Korhonen, O., Laitinen, R., 2012. Co-amorphous simvastatin and glipizide combinations show improved physical stability without evidence of intermolecular interactions. *Eur. J. Pharm. Biopharm.* 81, 159–169.

Lu, Q., Zografi, G., 1998. Phase behavior of binary and ternary amorphous mixtures containing indomethacin, citric acid and PVP. *Pharm. Res.* 15, 1202–1206.

MacFhionnghaile, P., Hu, Y., Gniado, K., Curran, S., McArdle, P., Erxleben, A., 2014. Effects of ball-milling and cryomilling on sulfamerazine polymorphs: a quantitative study. *J. Pharm. Sci.* 103, 1766–1778.

Masuda, T., Yoshihashi, Y., Yonemochi, E., Fujii, K., Uekusa, H., Terada, K., 2012. Cocrystallization and amorphization induced by drug–excipient interaction improves the physical properties of acyclovir. *Int. J. Pharm.* 422, 160–169.

Noyes, A.A., Whitney, W.R., 1897. The degree of the solution of solid substances in their solutions. *J. Am. Chem. Soc.* 19, 930–934.

Sobotka, H., Czczowiczka, N., 1958. The gelation of bile salt solutions. *J. Colloid Sci.* 13, 188–191.

Williams, H.D., Trevaskis, N.L., Charman, S.A., Shanker, R.M., Charman, W.N., Pouton, C.W., Porter, C.J.H., 2013. Strategies to address low drug solubility in discovery and development. *Pharmacol. Rev.* 65, 315-499.